NO and deuterium co-adsorption on the reconstructed Pt(100)-hex surface: A temperature programmed reaction study

ARTICLE *in* SURFACE SCIENCE · MAY 2000

Impact Factor: 1.93 · DOI: 10.1016/S0039-6028(00)00311-3

3 AUTHORS:

Evgeny Vovk
Boreskov Institute of Catalysis
32 PUBLICATIONS **141** CITATIONS
SEE PROFILE

Mikhail Yu. Smirnov
Boreskov Institute of Catalysis
48 PUBLICATIONS **494** CITATIONS
SEE PROFILE

Dmitry Zemlyanov
Purdue University
132 PUBLICATIONS **1,797** CITATIONS
SEE PROFILE

ELSEVIER

Surface Science 453 (2000) 103–111

surface science

www.elsevier.nl/locate/susc

NO and deuterium co-adsorption on the reconstructed Pt(100)-*hex* surface: a temperature programmed reaction study

E.I. Vovk *, M.Yu. Smirnov, D. Zemlyanov [1]

Boreskov Institute of Catalysis, Pr. Ak. Lavrentieva, 5, Novosibirsk 630090, Russia

Received 16 September 1999; accepted for publication 20 January 2000

Abstract

The deuterium adsorption at 270 K on a reconstructed Pt(100)-*hex* surface covered by NO_{ads} was studied by means of temperature programmed reaction (TPR). In the case of adsorption on a clean Pt(100)-*hex* surface the saturated D_{ads} coverage is 0.06 ML at $P_{H_2} = 6 \times 10^{-8}$ mbar, whereas the D_{ads} uptake is enhanced considerably by NO pre-adsorption. First the D_{ads} uptake increases with increasing NO_{ads} coverage, θ_{NO}, reaching a maximum at $\theta_{NO} \approx 0.25$ ML, and then decreases to zero. This phenomenon is explained as follows. The NO adsorption on the *hex* surface leads to the formation of 1×1 islands saturated by NO_{ads} and surrounded by the *hex* phase. The $NO_{ads}/1 \times 1$ islands are assumed to modify the *hex* phase adjacent to the island boundaries, adapting this area for deuterium adsorption.

TPR in the co-adsorption layer of NO_{ads} and D_{ads} is initiated by D_2 desorption and shows an 'explosive' behaviour, manifesting itself in the narrow TPR peaks of N_2 and D_2O at $\sim$370 K. The NO_{ads} pre-coverage affects the reaction temperature as well. Thus, at NO_{ads} coverage of 0.35–0.40 ML the temperature of the surface explosion increases abruptly by $\sim$15–20 K. At this coverage the $NO_{ads}/1 \times 1$ islands are supposed to modify the rest of the *hex* phase so that, after further D_2 adsorption, the surface becomes completely saturated by D_{ads} and NO_{ads} species. A possible mechanism for this is discussed.

Keywords: Deuterium; Hydrogen molecule; Nitrogen oxides; Platinum; Surface relaxation and reconstruction

1. Introduction

The Pt(100) surface is an attractive object for researchers in the field of heterogeneous catalysis due to the fact that a number of reactions on this surface, including $NO + H_2$, show fascinating phenomena such as sustained kinetic oscillations, propagation of periodic surface concentration waves, and 'surface explosions' [1,2]. The Pt(100) surface can exist in two different structures — a reconstructed hexagonal *hex* phase and an unreconstructed 1×1 phase; these can transform into each other depending on the temperature and chemical composition of the adsorption layer [3–5]. The *hex* and 1×1 surfaces exhibit dramatically different adsorption and catalytic properties.

The adsorption of hydrogen on unreconstructed Pt(100)-1×1 and reconstructed Pt(100)-*hex* surfaces has been studied in detail [6–15]. The adsorp-

* Corresponding author. Fax: +7-3832-343056.

E-mail addresses: vovk@catalysis.nsk.su (E.I. Vovk), dzem@wpi.edu (D. Zemlyanov)

[1] Present address: Worcester Polytechnic Institute, 100 Institute Road, Worcester, 01609 MA, USA.

0039-6028/00/$ - see front matter
PII: S0039-6028(00)00311-3

tion states and coverage of H_{ads} depend on the surface structure of Pt(100), temperature and hydrogen pressure. On the 1×1 surface, hydrogen adsorbs dissociatively occupying four-fold hollow and two-fold bridge adsorption sites [15]. The hydrogen uptake at 300 and 150 K reaches values of 0.6 and 1.20 ML[2] respectively [8,12].

The adsorption of hydrogen on the reconstructed surface lifts the *hex* reconstruction [8,10–12]. Since the rate of the *hex*$\rightarrow1\times1$ phase transition is proportional to the fourth power of the local coverage of hydrogen on the *hex* phase [13]; the rate of the hydrogen adsorption accompanying the phase transition depends strongly on the surface temperature and hydrogen pressure. Thus, H_{ads} coverage is about 0.05–0.1 ML at $\sim$300 K and $P_{H_2}\leq6\times10^{-8}$ mbar [7,12], whereas at 150 K θ_H can reach 1.20 ML [8]. The low temperature adsorption of hydrogen on the *hex* phase leads to the formation of four-fold hollow and bridge H_{ads} states, located on areas with a 1×1 structure and, in addition, one or several adsorption states populating structural defects, which are formed during the *hex*$\rightarrow1\times1$ reconstruction [15]. The amount of hydrogen populating the defects is about 20% of all the hydrogen adsorbed [15].

The adsorption of nitric oxide on the reconstructed surface at $T\leq300$ K lifts locally the *hex* reconstruction [5,8] forming islands of 1×1 structure populated with NO_{ads} molecules and surrounded by the hexagonal phase free of adsorbates [16]. The formation and growth of the $NO_{ads}/1\times1$ islands proceed through a nucleation and trapping mechanism. First nuclei are formed on the surface and then the islands grow on the basis of these nuclei [17]. The local coverage of NO_{ads} inside the growing islands is constant on NO adsorption and is about 0.5 ML, i.e. close to the saturation coverage on the 1×1 phase [16]. Two molecular adsorption states of NO are detected in the $NO_{ads}/1\times1$ islands [16,18–20]. A major state, denoted as $NO_{1\times1}$ occupies areas of the 1×1 structure and another state, denoted as NO_{def}, is located on structural defects formed during the *hex* $\rightarrow$ 1×1 reconstruction.

As discussed above, the adsorption of NO and H_2 on Pt(100)-*hex* and 1×1 surfaces is covered adequately but this is not the case for the co-adsorption of NO and hydrogen. The present work is aimed at studying the influence of the $NO_{ads}/1\times1$ islands on the hydrogen adsorption on the Pt(100)-*hex* surface. The adsorption of hydrogen (deuterium) is performed at 270 K and a partial pressure of 5.7×10^{-8} mbar, where H_{ads} coverage on the clean reconstructed Pt(100)-*hex* surface is negligible.

2. Experimental

The experiments were carried out in a stainless steel ultra-high vacuum chamber of an ADES-400 electron spectrometer (base pressure $\leq10^{-10}$ mbar). TPR spectra were obtained at a heating rate of 10 K/s by means of a VG QXK 400 quadrupole mass spectrometer. A self-designed processor controlled device was interfaced to the spectrometer for acquisition of the mass spectrometer data and for controlling the temperature and heating rate of the sample during the TPR experiments [21].

A Pt single crystal oriented along the (100) direction within $<0.5^\circ$ was used. The crystal was spot welded between two tantalum wires allowing to heat it up to 1200 K by passing a current through the wires. The temperature was measured by means of a Chromel/Alumel thermocouple spot welded to an edge side of the single crystal. Circulation of liquid nitrogen through a reservoir in thermal contact with the sample holder allowed the crystal to be cooled to 100 K. The cleaning procedure included cycles of Ar^+ ion etching and subsequent annealing in oxygen and in vacuum. The clean Pt(100) surface exhibited a (5×20) low energy electron diffraction pattern characteristic for the reconstructed *hex* surface. D_2 and ^{15}NO were used for the TPR experiments in order to increase the reliability of the identification of the products by mass spectrometry.

The coverages of NO_{ads} and D_{ads} were estimated from areas under the thermal desorption peaks in

[2] A monolayer (ML) is equated to the density of platinum atoms in the topmost layer of the Pt(100)-1×1 surface, 1.28×10^{15} cm^{-2}.

regards to the corresponding value for the saturated adlayers. In the case of NO_{ads}, the products of NO dissociation in the course of TPR were taken into account. It was assumed that the saturation coverage of NO_{ads} at 300 K on the Pt(100)-*hex* surface was 0.5 ML [16]. The deuterium coverage was referred to that of the saturated D_{ads} layer prepared on the Pt(100)-*hex* surface at 150 K, which is equal to 1.2 ML [8]. The exposure was measured in mbar·s taking into account the ionisation cross-sections of NO and deuterium to be 1.3 and 0.35 respectively.

3. Results

Fig. 1 shows typical TPR spectra obtained after an exposure of the Pt(100)-*hex* surface containing the $NO_{ads}/1\times1$ islands to D_2 at 270 K. The D_{ads} uptake is significantly bigger than that measured after D_2 adsorption on the clean *hex* surface, shown in Fig. 1 by the dotted line. Moreover, the desorption of D_2O points to the fact that some

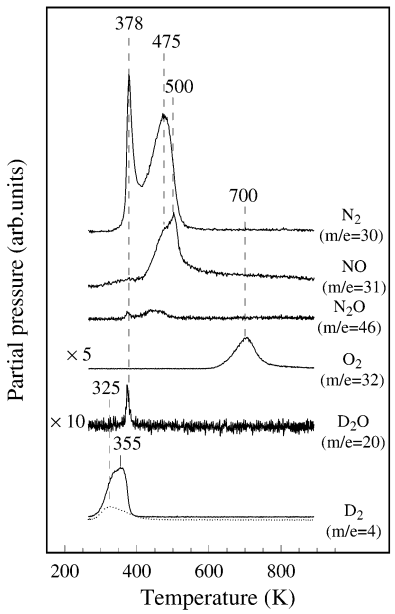

Fig. 1. TPR spectra taken after exposure of the Pt(100) surface covered with 0.37 ML of NO (solid lines), and the clean Pt(100)-*hex* surface (dotted line) to 4.3×10^{-5} mbar·s of D_2 at 270 K.

D_{ads} is consumed under heating due to reaction with NO_{ads}. The products of the reaction between D_{ads} and NO_{ads}, such as D_2O and N_2, desorb as narrow peaks at ~375 K with full width at half maximum ~10–15 K. This phenomenon has been called 'surface explosion' in the literature and it reflects an autocatalytic character of the reaction [22]. D_2 desorption completes abruptly with development of the surface explosion. An unreacted remainder of NO_{ads} desorbs as NO, and the products related to NO_{ads} dissociation such as N_2, O_2 and N_2O [23,24]. Summarising, the significant desorption of D_2 and D_2O (the latter resulting from the $NO_{ads}+D_{ads}$ reaction) points to the fact that the Pt(100)-*hex* surface, containing the $NO_{ads}/1\times1$ islands, absorbs deuterium in amounts exceeding the saturated coverage on a clean Pt(100)-*hex* surface at 270 K.

Fig. 2 shows $^{15}N_2$ TPR spectra taken from NO_{ads} layers with two different θ_{NO} exposed to D_2. In both cases $^{15}N_2$ desorbs as two peaks. The first narrow peak at 365–380 K is due to the reaction between NO_{ads} and D_{ads}, and the second one at ~470 K is attributed to the dissociation of the rest of NO_{ads}. The intensity of the sharp 'reaction' N_2 peak increases gradually with D_2 exposure, whereas the desorption peak at ~470 K is slightly attenuated, indicating the progress of the reaction between NO_{ads} and deuterium. This conclusion is also supported by the simultaneous increase of the intensity of the D_2O peak (not shown here). The contribution of the sharp reaction peak to the total yield of N_2 is lower at $\theta_{NO}=0.4$ ML.

Fig. 3 shows the areas under the D_2 desorption and N_2 reaction peaks as a function of D_2 exposure for various θ_{NO} coverage. The areas of the N_2 and D_2 peaks reflecting the kinetics of D_{ads} accumulation with D_2 exposure show a similar behaviour for all values of θ_{NO}. D_{ads} coverage increases quickly with D_2 exposure and then, after exposure of 1.4×10^{-5} mbar·s, grows slowly. A careful examination of the curves plotted in Fig. 3 points to the fact that the yields of N_2 and D_2, and consequently the D_{ads} uptake, are non-monotonic functions of θ_{NO}. Thus, the D_{ads} uptake increases with θ_{NO} so long as the NO_{ads} coverage is less than 0.25 ML. Under further increase of θ_{NO}, D_{ads} coverage decreases gradually. Deuterium does not adsorb on the surface saturated by NO_{ads}

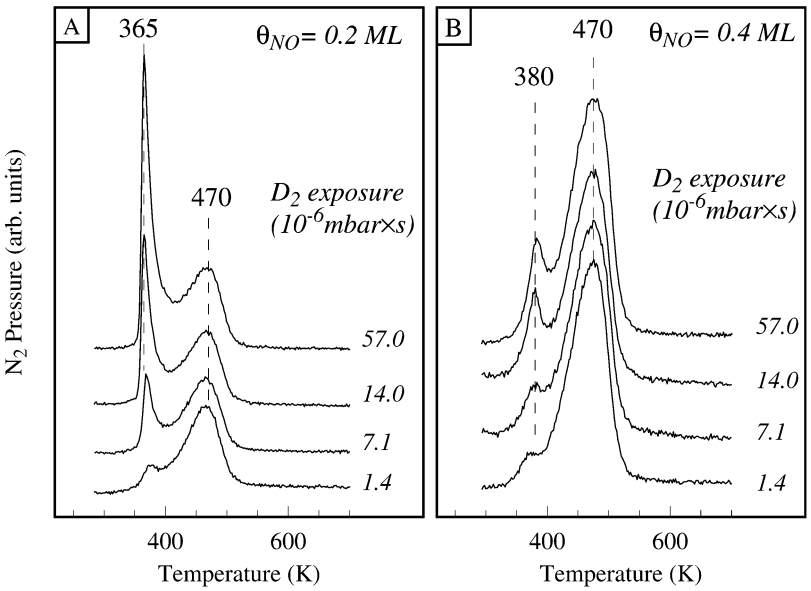

Fig. 2. TPR spectra of $^{15}N_2$ ($m/e=30$) depending on exposures of the Pt(100)-*hex* surface covered with (A) 0.2 and (B) 0.4 ML of NO_{ads} to D_2 at 270 K.

($\theta_{NO}=0.5$ ML [16,25]). Fig. 4 shows TPR spectra of N_2 and D_2 taken after an exposure of NO_{ads} layers with various θ_{NO} on Pt(100)-*hex* to 1.4×10^{-5} mbar·s of D_2. These data are represented quantitatively in Fig. 5. One can see that the D_{ads} uptake shows a maximum at $\theta_{NO}\approx0.25$ ML.

The temperature of the surface explosion shows a dependence on NO_{ads} pre-coverage as well (Fig. 4A). Thus, at $\theta_{NO}\approx0.35$–0.4 ML the maximum of the N_2 reaction peak shifts abruptly towards higher temperatures by $\sim$15–20 K (Fig. 6A). The onset temperature of D_2 desorption increases abruptly by $\sim$15–20 K at the same θ_{NO} as well (Fig. 6B). The onset temperature was determined by the point where a tangent line to the forward front of D_2 desorption peak in the inflection point intersects the background level.

4. Discussion

4.1. Morphology of NO_{ads} and D_{ads} co-adsorption layers on the Pt(100)-hex surface

As demonstrated in the present work, the *hex* surface covered with the $NO_{ads}/1\times1$ islands can offer some adsorption sites for the adsorption of D_2 and that is very unlikely for a clean Pt(100)-*hex* surface. One can suggest that these sites are located inside the $NO_{ads}/1\times1$ islands. However, our previous studies [20,26,27] showed that if some vacant sites exist inside the $NO_{ads}/1\times1$ islands for hydrogen adsorption, then H_2 reacts with NO_{ads} at 300 K, yielding N_2 and H_2O, without the formation of a stable NO/H co-adsorption layer. Moreover, if the formation of the co-adsorption $(NO_{ads}+H_{ads})/1\times1$ islands really takes place, it should lead to a gradual increase of the D_{ads} uptake with increasing θ_{NO} reaching a maximum near the saturated NO_{ads} coverage. This is not the case, as shown in Fig. 5. Another suggestion is that the $NO_{ads}/1\times1$ islands create some adsorption sites for deuterium in the boundary regions around the islands. Indeed, the *hex* phase adjacent to the boundaries of the islands is distorted due to the difference in the structure and atomic density of the 1×1 and *hex* phases and, therefore, this area could be adapted for D_2 adsorption. D_{ads} covered areas affect the surrounding *hex* phase to much lesser extent than the $NO_{ads}/1\times1$ islands. For instance, on the non-homogeneous Pt(100) surface, containing both the 1×1 and *hex* phases,

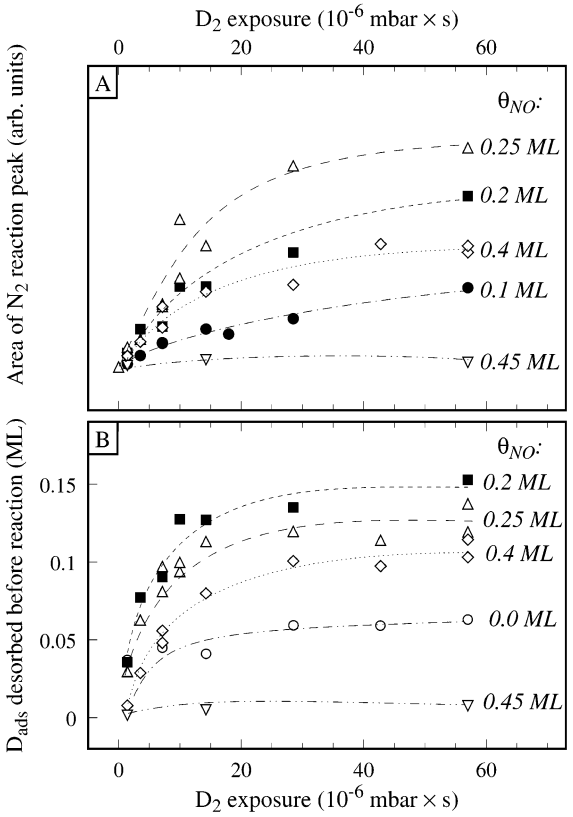

Fig. 3. Areas of: (A) the $^{15}N_2$ reaction peak; and (B) the deuterium desorption peak as functions of D_2 exposure for various NO_{ads} coverage.

D_{ads} populates only the 1×1 phase at 300 K and does not extend the adsorption on the *hex* phase [28]. Consequently, it is suggested that D_{ads} occupies limited areas around the $NO_{ads}/1\times1$ islands, however, it does not affect the surrounding *hex* phase strongly enough for further adaptation of all the residual *hex* surface for deuterium adsorption.

The hypothesis about D_{ads} location in ring-like areas around the $NO_{ads}/1\times1$ islands is consistent with the non-monotonic variation of the D_{ads} uptake with θ_{NO} coverage. According to the nucleation and trapping mechanism for the adsorption island formation on the Pt(100)-*hex* surface [17,29], the initial stage of nuclei creation is followed by a stage of island growth on the basis of these nuclei, practically without change of the island number. The mean size of the islands increases with the θ_{NO} coverage. In the beginning, the ring-like area should increase with the growth of the $NO_{ads}/1\times1$ island, enlarging the surface available for D_2 adsorption. However, with further island growth, the ring-like areas overlap and this is responsible for the decrease in the area adapted for deuterium adsorption. A simplified model of D_2 adsorption around the $NO_{ads}/1\times1$ islands is considered in the Appendix. The model is based on the assumption that all the original $NO_{ads}/1\times1$ islands are round in shape and equal in radius. The model predicts a non-monotonic dependence of the D_{ads} uptake on NO_{ads} coverage, which is close to the experimental one (compare Figs. 5 and 8).

However, one can suggest that D_{ads} adsorption around the $NO_{ads}/1\times1$ islands on the distorted area might be accompanied by a mixing of D_{ads} and NO_{ads} through a slow exchange of adsorption sites. For instance, the subsequent adsorption of NO and CO on the Pt(100)-*hex* surface results in the formation of the mixed islands $(NO_{ads}+CO_{ads})/1\times1$ [30]. On the other hand, there are several examples where two co-adsorbed species segregate into separate phases of individual adsorbates: H_{ads} and CO_{ads} on Pt(111) [31,32], Ni(111) [33] and Rh(100) [34,35]. Here, we supposed that the mixing of D_{ads} and NO_{ads} did not happen or was a very slow process. In any case, further investigations are necessary to elucidate a spatial distribution of D_{ads} and NO_{ads} species inside the co-adsorption island, as well as on the nature of the distorted area.

4.2. The influence of the $NO_{ads}/1\times1$ island size on the $NO_{ads}+D_{ads}$ reaction temperature

As shown in Fig. 2, the temperature of the explosive evolution of N_2 practically does not depend on D_2 exposure, whereas it demonstrates a dependence on the NO_{ads} pre-coverage (Figs. 4 and 6A). The steep increase of the reaction temperature, by $\sim$15–20 K is observed at $\theta_{NO}=0.35$–0.4 ML. It is quite remarkable that the onset temperature of D_2 desorption shows the same behaviour (Fig. 6B). The similar behaviour of

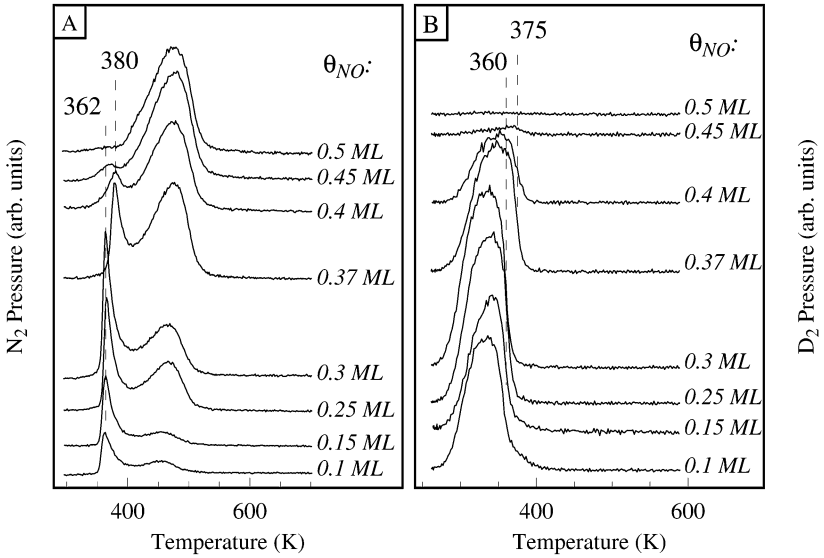

Fig. 4. TPR spectra of: (A) $^{15}N_2$; and (B) D_2 taken after an exposure of NO_{ads} layers on Pt(100)-*hex* with various coverage to 1.4×10^{-5} mbar·s of D_2 at 270 K.

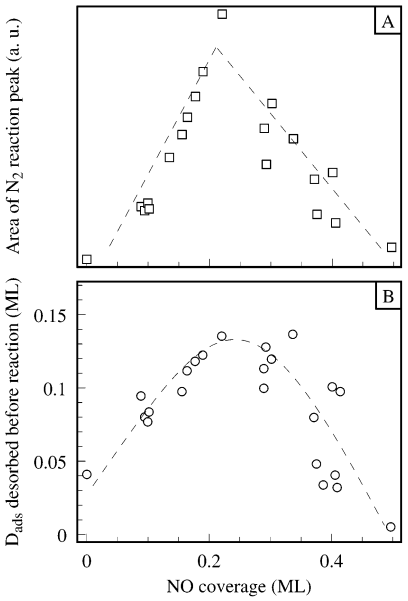

Fig. 5. (A) The area of the reaction peak of $^{15}N_2$; and (B) the amount of D_{ads} desorbed before the reaction as functions of the initial coverage of NO_{ads}. The represented data were obtained for an exposure to 1.4×10^{-5} mbar·s of D_2 or higher.

these temperatures could be explained based on the general mechanism of surface explosion reactions on Pt(100) proposed in Ref. [25]. According to this mechanism, D_2 desorption initiates the explosive reaction between NO_{ads} and D_{ads}, and therefore the increase in the temperature of D_2 desorption should lead to an increase in the reaction temperature. The theoretical simulation of the desorption process from the heterogeneous surface showed a shift of the desorption temperature, depending on the surface phase composition [36]. The unusual temperature shift of D_2 desorption represented in Fig. 6 could be assigned to the change in a qualitative phase composition of the surface. At low θ_{NO} pre-coverage followed by saturation with deuterium, some part of the surface has the *hex* structure, which is free of adsorbed species. As the θ_{NO} pre-coverage increases, the contribution of the *hex* phase, retaining free after the consequent D_2 adsorption, decreases gradually. When the free *hex* phase disappears completely, the desorption temperature of D_2 increases steeply. Since D_2 desorption initiates the reaction between NO_{ads} and D_{ads}, a steep temperature increase of D_2 desorption results in the increase of reaction temperature.

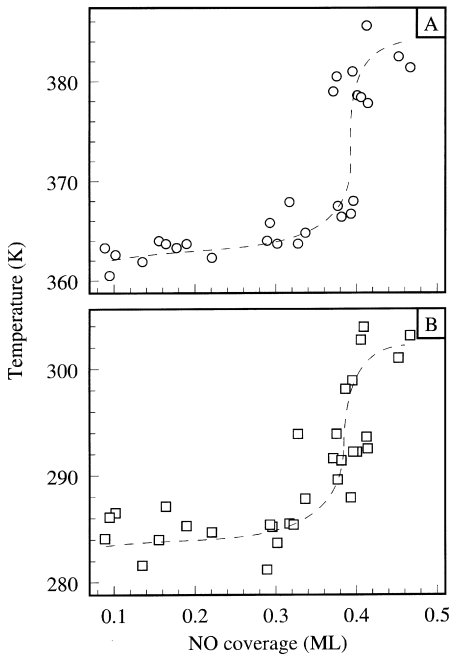

Fig. 6. (A) The temperature of the reaction peak of N_2, and (B) the onset temperature of D_2 desorption as functions of NO_{ads} coverage. The temperature of D_2 desorption is determined as the point of intersection of a tangent line of the forward front of D_2 desorption curve in the inflection point and a background level. The represented data are for D_2 exposure of 1.4×10^{-5} mbar·s or higher.

5. Conclusion

The $NO_{ads}/1\times1$ islands on the Pt(100)-*hex* surface can significantly increase the D_{ads} (H_{ads}) uptake at 270 K. The $NO_{ads}/1\times1$ islands are supposed to modify the surrounding *hex* phase. The modification extends over a limited part of the *hex* phase adjacent to the boundaries of the islands which is responsible for the non-monotonic variation of the adsorption capacity towards deuterium with the θ_{NO} pre-coverage.

Appendix

Let us assume that at any given NO_{ads} coverage all the $NO_{ads}/1\times1$ islands are round in shape and uniform in size, and the number of the islands n is independent of θ_{NO}. Another assumption is that there is a ring area of width d around the $NO_{ads}/1\times1$ islands of radius r which is able to adsorb deuterium. The problem is to infer the portion of the surface S_D covered with the D_{ads} rings as a function of the θ_{NO} coverage with regard to a possible overlap of the rings.

A solution to the problem is performed taking an approach developed by Mampel for modelling the kinetics of heterogeneous reactions on solid surfaces [37]. This approach holds that a portion of the surface free of the adsorption islands is equal to the probability that a randomly chosen point A on the surface is not covered by any of n disks of radius r thrown randomly on the surface. The probability is derivable from Poisson statistics, so that the probability of m coverings of point A from n attempts is

$$W(m,r)=\frac{1}{m!}(n\pi r^2)^m\exp(-n\pi r^2). \tag{A1}$$

Substituting $m=0$ in Eq. (A1) gives the portion of the surface which is free of the $NO_{ads}/1\times1$ islands:

$$S_{free}=W(0,r)=\exp(-n\pi r^2). \tag{A2}$$

The portion covered with $NO_{ads}/1\times1$ islands is expressed as

$$S_{NO}=2\theta_{NO}=1-\exp(-n\pi r^2). \tag{A3}$$

Here, it is accounted for that the saturation of the 1×1 phase is reached at $\theta_{NO}=0.5$ ML [16,25]. The radius of the $NO_{ads}/1\times1$ islands is derivable as a function of θ_{NO} from Eq. (A3):

$$r=\frac{1}{\sqrt{n\pi}}\ln^{1/2}\frac{1}{1-2\theta_{NO}}. \tag{A4}$$

Once deuterium adsorbs on the surface, the islands contain both NO_{ads} and D_{ads}, and their radius is equal to $r+d$. The portion of the surface covered with D_{ads} is expressed by the difference of two probabilities:

$$\begin{aligned}S_D&=W(0,r)-W(0,r+d)\\&=\exp(-n\pi r^2)-\exp[-n\pi(r+d)^2].\end{aligned} \tag{A5}$$

Substitution of Eq. (A4) into Eq. (A5) gives:

$$S_D = (1-2\theta_{NO})\left\{1-\exp(-n\pi d^2)\times\exp\left(-2d\sqrt{n\pi}\ln^{1/2}\frac{1}{1-2\theta_{NO}}\right)\right\}. \quad (A6)$$

To yield S_D as a function of n and θ_{NO} only, a relationship between the width of the D_{ads} rings and the radius of the $NO_{ads}/1\times1$ islands, $d(r)$, is required to be entered into Eq. (A6). It is expected that the $d(r)$ function possesses the following properties: it grows monotonically with r, and has a finite limit $d_0 = \lim_{r\to\infty} d(r)$. Without other particular characteristics of the $d(r)$ function, we arbitrarily prescribed the function as:

$$d(r) = d_0(1-e^{-ar}), \quad (A7)$$

which complies with the requirements. Here, a is a parameter determining the rate of d growth at lowest values of r. Fig. 7 demonstrates a set of functions (A7) with varying parameter a. Fig. 8 shows two series of S_D–θ_{NO} relationships obtained after the substitution of the $d(r)$ function (A7) into Eq. (A6) with variation of a-parameter at d_0 = constant (Fig. 8A) and with variation of d_0 at a = constant (Fig. 8B). The relationships in Fig. 8 are built up assuming that the concentration of the islands $n = 10^{10}$ cm^{-2}, from that reasoning that a typical size for the adsorption islands formed under the saturation of the Pt(100)-*hex* surface is about 1000Å [13,29,38].

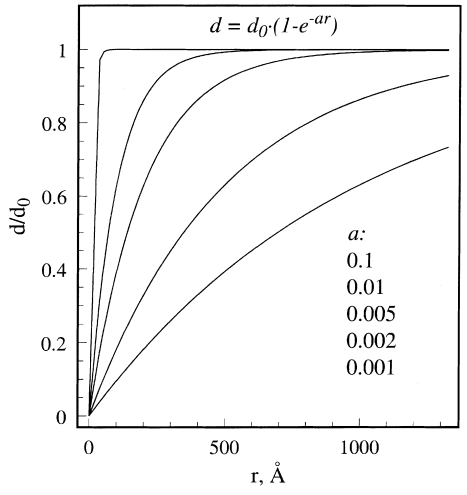

Fig. 7. The function of $d(r)$ depending of the value of the a-parameter.

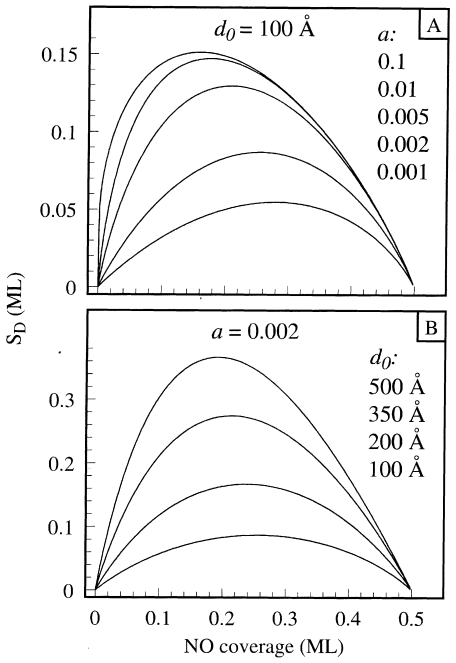

Fig. 8. The variations of the relationship between S_D and θ_{NO}: (A) with the a-parameter at $d_0 = 100$ Å; and (B) with d_0 at $a = 0.002$.

All the S_D–θ_{NO} relationships shown in Fig. 8 pass through a maximum which falls in the interval of the NO_{ads} coverage between 0.15 and 0.3 ML at the given limits of a and d_0 variations. S_D exhibits a reasonable order of magnitude in the vicinity of the θ_{NO} coverage expected from the experimental data obtained. It is believed that an adequate description of the experimental relationship between the amount of deuterium adsorbed and θ_{NO} coverage could be accomplished through the a and d_0 parameters.

References

[1] R. Imbihl, Prog. Surf. Sci. 44 (1993) 185.
[2] M.M. Slin'ko, N.I. Jaeger, in: Oscillating Heterogeneous Catalytic Systems, Studies in Surface Science and Catalysis Vol. 86 Elsevier, Amsterdam, 1994.
[3] J.J. McCarroll, Surf. Sci. 53 (1975) 297.

[4] P. Heilmann, K. Heinz, K. Müller, Surf. Sci. 83 (1979) 487.
[5] H.P. Bonzel, G. Broden, G. Pirug, J. Catal. 53 (1978) 96.
[6] K.E. Lu, L.L. Rye, Surf. Sci. 45 (1974) 677.
[7] M.A. Barteau, E.I. Ko, R.J. Madix, Surf. Sci. 102 (1981) 99.
[8] P.R. Norton, J.A. Davies, D.K. Creber, C.W. Sitter, T.E. Jackman, Surf. Sci. 108 (1981) 205.
[9] V.A. Sobyanin, V.P. Zhdanov, Surf. Sci. 181 (1987) L163.
[10] B. Pennemann, K. Oster, K. Wandelt, Surf. Sci. 249 (1991) 35.
[11] J. Radnik, F. Gitmans, B. Pennemann, K. Oster, K. Wandelt, Surf. Sci. 287/288 (1993) 330.
[12] B. Klötzer, E. Bechtold, Surf. Sci. 295 (1993) 374.
[13] A.T. Pasteur, St.J. Dixon-Warren, D.A. King, J. Chem. Phys. 103 (1995) 2251.
[14] Ch. Romanczyk, J.R. Manson, K. Kern, K. Kuhnke, R. David, P. Zeppenfield, G. Comsa, Surf. Sci. 336 (1995) 362.
[15] D.Yu. Zemlyanov, M.Yu. Smirnov, V.V. Gorodetskii, Catal. Lett. 43 (1997) 181.
[16] P. Gardner, M. Tüshaus, R. Martin, A.M. Bradshaw, Surf. Sci. 240 (1990) 112.
[17] E. Ritter, R.J. Behm, G. Pötschke, J. Wintterlin, Surf. Sci. 181 (1987) 403.
[18] G. Pirug, H.P. Bonzel, H. Hopster, H. Ibach, J. Chem. Phys. 71 (1979) 593.
[19] D.Yu. Zemlyanov, M.Yu. Smirnov, React. Kinet. Catal. Lett. 53 (1994) 97.
[20] D.Yu. Zemlyanov, M.Yu. Smirnov, V.V. Gorodetskii, J.H. Block, Surf. Sci. 329 (1995) 61.
[21] V.V. Kaichev, A.M. Sorokin, A.M. Badalyan, D.Yu. Nikitin, O.V. Moskovkin, Instrum. Exp. Tech. 40 (1997) 575.
[22] M.W. Lesley, L.D. Schmidt, Surf. Sci. 155 (1985) 215.
[23] R.J. Gorte, L.D. Schmidt, J.L. Gland, Surf. Sci. 109 (1981) 367.
[24] D.Yu. Zemlyanov, M.Yu. Smirnov, V.V. Gorodetskii, React. Kinet. Catal. Lett. 53 (1994) 87.
[25] Th. Fink, J.-P. Dath, M.R. Basset, R. Imbihl, G. Ertl, Surf. Sci. 245 (1991) 96.
[26] D.Yu. Zemlyanov, M.Yu. Smirnov, V.V. Gorodetskii, Catal. Lett. 28 (1994) 153.
[27] D.Yu. Zemlyanov, M.Yu. Smirnov, V.V. Gorodetskii, Phys. Low-Dimen. Struct. 4/5 (1994) 89.
[28] D.Yu. Zemlyanov, M.Yu. Smirnov, E.I. Vovk, Langmuir 15 (1999) 135.
[29] A. Borg, A.M. Hilmen, E. Bergene, Surf. Sci. 306 (1994) 10.
[30] M.Yu. Smirnov, D.Yu. Zemlyanov, V.V. Gorodetskii, E.I. Vovk, Surf. Sci. 414 (1998) 409.
[31] D. Hoge, M. Tüshaus, A.M. Bradshaw, Surf. Sci. 207 (1989) L935.
[32] M.Yu. Smirnov, V.V. Gorodetskii, A.R. Cholach, D.Yu. Zemlyanov, Surf. Sci. 313 (1994) 308.
[33] G.E. Mitchel, J.L. Gland, Surf. Sci. 131 (1983) 167.
[34] L.J. Richter, B.A. Gurney, W. Ho, J. Chem. Phys. 86 (1987) 477.
[35] D.E. Peebles, H.C. Peebles, J.M. White, Surf. Sci. 136 (1984) 463.
[36] V.I. Savchenko, Kinet. Catal. 35 (1994) 316.
[37] P. Barret, Cinetique Heterogene, Gauthier-Villars, Paris, 1973.
[38] A. Hopkinson, X.-C. Guo, J.M. Bradley, D.A. King, J. Chem. Phys. 99 (1993) 8264.